Many-Body Nonlocality as a Resource for Quantum-Enhanced Metrology

Artur Niezgoda and Jan Chwedeńczuk
Faculty of Physics, University of Warsaw, Ulica Pasteura 5, PL–02–093 Warszawa, Poland

(Received 5 February 2021; accepted 4 May 2021; published 28 May 2021)

We demonstrate that the many-body nonlocality witnessed by a broad family of Bell inequalities is a resource for ultraprecise metrology. We formulate a general scheme which allows one to track how the sensitivity grows with the nonlocality extending over an increasing number of particles. We illustrate our findings with some prominent examples—a collection of spins forming an Ising chain and a gas of ultracold atoms in any two-mode configuration. We show that in the vicinity of a quantum critical point the rapid increase of the sensitivity is accompanied by the emergence of the many-body Bell nonlocality. The method described in this work allows for a systematic study of highly quantum phenomena in complex systems, and also extends the understanding of the beneficial role played by fundamental nonclassical effects in implementations of quantum-enhanced protocols.

DOI: 10.1103/PhysRevLett.126.210506

The triad of quantum phenomena, i.e., entanglement [1], Einstein-Podolsky-Rosen steering [2–4], and Bell nonlocality [5,6], plays a pivotal role in our understanding of quantum mechanics and can improve the performance of various protocols like quantum cryptography [7–11] or quantum computing [12,13]. Entanglement drives the other two phenomena—it is necessary, though not sufficient, to observe the steering or nonlocality. For instance, the four two-qubit Bell states are all maximally entangled. For quantum-enhanced metrology, entanglement is the resource for breaking the shot-noise limit [14,15] and recently it has been demonstrated that it is possible to steer a quantum sensor to improve its sensitivity [16]. In this context, Bell correlations can also be an asset, as has been shown in some cases [17–19]. Bell correlations and nonlocality have been observed with photons [20–30], Josephson qubits [31], or massive particles [32–35], and quantum-enhanced sensors operating on many-body systems have been realized in many configurations [36–41].

Here we develop a general framework which allows one to link the many-body nonlocality with the sensitivity of a quantum sensor in a systematic way. We derive a lower bound for the quantum Fisher information (QFI), the central object in quantum metrology [42–44], in terms of a series of Bell correlators of all orders. We demonstrate that the many-body nonlocality detected by these correlators is *sufficient* to reach very high sensitivities, i.e., it is a resource for ultraprecise metrology. These general results are corroborated by the examples of the QFI and the Bell correlators calculated with an Ising chain [45,46] and the Bose-Einstein condensate in the double-well potential [47–49]. In both examples, we observe that in the proximity of a critical point the swift gain of precision is driven by the nonlocality that spreads over an increasing number of particles. Knowledge of the relation between the nonlocality and metrology may prove important for these two areas of research and for our understanding of many-body quantum mechanics.

We rely on a model of local realism that takes N parties, and each party independently measures two quantities $\sigma_{1/2}^{(k)}$ which give binary (± 1) outcomes. We construct an N-party (N-body or N-particle) correlator from an ensemble average of a product of outcomes

$$\mathcal{E}_{\vec{n}_+,\vec{n}_-} = \left| \left\langle \prod_{k=1}^{N} \sigma_{\pm}^{(k)} \right\rangle \right|^2, \tag{1}$$

where $\sigma_{\pm}^{(k)} = \frac{1}{2}(\sigma_1^{(k)} \pm i\sigma_2^{(k)})$. The labels $\vec{n}_+$ and $\vec{n}_-$ inform which n_+ parties picked the $+$ or the $-$ sign ($n_- = N - n_+$). If this average is consistent with the postulates of local realism, it can be expressed as

$$\begin{aligned} \mathcal{E}_{\vec{n}_+,\vec{n}_-} &= \left| \int d\lambda p(\lambda) \prod_{k=1}^{N} \sigma_{\pm}^{(k)}(\lambda) \right|^2 \\ &\leq \int d\lambda p(\lambda) \prod_{k=1}^{N} |\sigma_{\pm}^{(k)}(\lambda)|^2 = 2^{-N}, \end{aligned} \tag{2}$$

where λ is a hidden variable and $p(\lambda)$ is its probability distribution. Therefore $\mathcal{E}_{\vec{n}_+,\vec{n}_-} \leq 2^{-N}$ is the many-body Bell inequality well suited to test the nonlocality in multiqubit systems [50–53].

For quantum systems, the correlator from Eq. (1) is an average of a product of n_+ rising and n_- lowering spin-1/2 operators. The information about the nonlocality is encoded in a single element of the density matrix that governs the $\uparrow - \downarrow$ coherence of the set of $\vec{n}_+$ qubits and the $\downarrow - \uparrow$ coherence of other $\vec{n}_-$ [54,55]. Every off-diagonal element

ϱ_{nm} of the density operator is bounded by $|\varrho_{nm}|^2 \leq \frac{1}{4}$, so $\mathcal{E}_{\vec{n}_+,\vec{n}_-} \leq \frac{1}{4}$ and the values of $\mathcal{E}_{\vec{n}_+,\vec{n}_-}$ between 2^{-N} and $\frac{1}{4}$ carry detailed information about the depth of nonlocality. When $\mathcal{E}_{\vec{n}_+,\vec{n}_-} \in]2^{-N}, 2^{-(N-1)}]$, the correlator can be reproduced with a model, where three out of N qubits are Bell correlated. When $\mathcal{E}_{\vec{n}_+,\vec{n}_-} \in]2^{-(N-1)}, 2^{-(N-2)}]$, the nonlocality extends over four qubits. Finally, when $\mathcal{E}_{\vec{n}_+,\vec{n}_-} \in]\frac{1}{8}, \frac{1}{4}]$, all N qubits are Bell correlated. Following this scheme, the extension of nonlocality over the many-body system can be tracked in a systematic way.

We now consider the scenario where the qubits undergo a metrological transformation, parameterized by θ (such as the relative phase between the arms of an interferometer or between the two levels in atomic clocks). We demonstrate that the sensitivity $\Delta\theta$ with which θ can be estimated is related to those correlators $\mathcal{E}_{\vec{n}_+,\vec{n}_-}$ with all combinations of $\vec{n}_+$ and $\vec{n}_-$. This way, we establish a link between quantum metrology and the nonlocality.

Consider a quantum system (here in its spectral form)

$$\hat{\varrho} = \sum_j p_j |\psi_j\rangle\langle\psi_j|. \tag{3}$$

The evolution—for instance a passage through an interferometer that introduced the dependence on θ—in the parameter space reads

$$i\partial_\theta \hat{\varrho} = [\hat{h}, \hat{\varrho}]. \tag{4}$$

For many quantum sensors the generator $\hat{h}$ takes the form of

$$\hat{h} = \frac{1}{2}\sum_{k=1}^{N} \hat{\sigma}_\xi^{(k)}, \tag{5}$$

where $\hat{\sigma}_\xi^{(k)}$ is a Pauli matrix of the kth qubit oriented along the axis $\vec{\xi} = (\xi_x, \xi_y, \xi_z)$, namely,

$$\hat{\sigma}_\xi^{(k)} = \xi_x \hat{\sigma}_x^{(k)} + \xi_y \hat{\sigma}_y^{(k)} + \xi_z \hat{\sigma}_z^{(k)}, \qquad (\vec{\xi})^2 = 1. \tag{6}$$

This collective generator (5) represents a wide family of interferometric transformations. For instance $\xi = y$ corresponds to the Mach-Zehnder interferometer with light or atoms or a Ramsey interferometric sequence employed in atomic clocks while $\xi = z$ stands for a phase shift.

All protocols of estimating θ have the sensitivity $\Delta\theta$ bounded by

$$\Delta\theta \geq \frac{1}{\sqrt{F_q}}. \tag{7}$$

This is the Cramér-Rao lower bound and the F_q is the QFI [42–44], which expressed in terms of the eigenstates and the corresponding eigenvalues of $\hat{\varrho}$ [see Eq. (3)] reads

$$F_q = 2\sum_{i,j} \frac{(p_i - p_j)^2}{p_i + p_j} |\langle\psi_i|\hat{h}|\psi_j\rangle|^2. \tag{8}$$

By putting $(p_i - p_j)^2$ under the absolute value and using $\hat{\varrho}|\psi_i\rangle = p_i|\psi_i\rangle$ [a consequence of Eq. (3)], we get

$$|\langle\psi_i|p_i\hat{h} - \hat{h}p_j|\psi_j\rangle|^2 = |\langle\psi_i|\hat{\varrho}\,\hat{h} - \hat{h}\,\hat{\varrho}\,|\psi_j\rangle|^2 \tag{9}$$

and hence

$$F_q = 2\sum_{i,j} \frac{1}{p_i + p_j} |\langle\psi_i|[\hat{\varrho}, \hat{h}]|\psi_j\rangle|^2. \tag{10}$$

Since $p_i + p_j \leq 1$, by neglecting the term in the denominator we obtain the lower bound

$$F_q \geq 2\sum_{i,j} |\langle\psi_i|[\hat{\varrho}, \hat{h}]|\psi_j\rangle|^2, \tag{11}$$

which leads to [54]

$$F_q \geq 4(\mathrm{Tr}[\hat{\varrho}^2\hat{h}^2] - \mathrm{Tr}[(\hat{\varrho}\,\hat{h})^2]). \tag{12}$$

This relation between the QFI and the Hilbert-Schmidt quantum statistical speed [56] is a first step towards establishing a link between the sensitivity and the many-body nonlocality.

The eigenstates of a single-qubit operator from Eq. (6) are $\hat{\sigma}_\xi^{(k)}|\uparrow/\downarrow\rangle_k = \pm 1|\uparrow/\downarrow\rangle_k$ and we represent the density matrix with a basis of N-qubit states $|n\rangle$ being a product of such eigenstates

$$\hat{\varrho} = \sum_{n,m=1}^{2^N} \varrho_{nm}|n\rangle\langle m|. \tag{13}$$

Here n, m run through all the combinations of $\uparrow$ and $\downarrow$ independently for each qubit. The basis state $|n\rangle$ is an eigenstate of $\hat{h}$,

$$\hat{h}|n\rangle = \left(n_\uparrow - \frac{N}{2}\right)|n\rangle, \tag{14}$$

where $n_\uparrow$ is the number of $|\uparrow\rangle$ qubits in $|n\rangle$. Each eigenstate of $\hat{h}$ is $\binom{N}{n_\uparrow}$ times degenerate, which is a consequence of the collective character of the generator from Eq. (5). Using the property Eq. (14), we obtain the expression for the lower bound of the QFI from Eq. (12) in the following form [54]:

$$F_q \geq 2\sum_{n,m} (n_\uparrow - m_\uparrow)^2 |\varrho_{nm}|^2. \tag{15}$$

We now focus on a single term of this sum and notice that every $|m\rangle$ can be obtained from any $|n\rangle$ by acting a proper

number of times with a rising (n_+) and lowering (n_-) operator, namely,

$$|m\rangle = \hat{\mathcal{R}}_{\vec{n}_+}\hat{\mathcal{L}}_{\vec{n}_-}|n\rangle \tag{16}$$

so that $m_\uparrow = n_\uparrow + n_+ - n_-$, giving

$$\varrho_{nm} = \langle n|\hat{\varrho}\hat{\mathcal{R}}_{\vec{n}_+}\hat{\mathcal{L}}_{\vec{n}_-}|n\rangle. \tag{17}$$

By $\hat{\mathcal{R}}$ and $\hat{\mathcal{L}}$ we denote a product of rising or lowering operators

$$\hat{\mathcal{R}}_{\vec{n}_+} = \hat{\sigma}_+^{(i_1)}\ldots\hat{\sigma}_+^{(i_{n_+})} \tag{18a}$$

$$\hat{\mathcal{L}}_{\vec{n}_-} = \hat{\sigma}_-^{(j_1)}\ldots\hat{\sigma}_-^{(j_{n_-})}, \tag{18b}$$

where for two directions orthogonal to $\vec{\xi}$, $\vec{\xi}_1$, and $\vec{\xi}_2$,

$$\hat{\sigma}_\pm^{(k)} = \frac{1}{2}(\hat{\sigma}_{\xi_1}^{(k)} \pm i\hat{\sigma}_{\xi_2}^{(k)}). \tag{19}$$

The vector symbol $\vec{n}_\pm$ in Eq. (16) indicates that $n_\pm$ qubits are risen or lowered and that they form a particular ordered subset of all possible choices from N qubits.

We now pick all the basis states $|n\rangle$ and $|m\rangle$, which are transformed one into another with given $\hat{\mathcal{R}}_{\vec{n}_+}$ and $\hat{\mathcal{L}}_{\vec{n}_-}$, leaving the other $N-(n_+ + n_-)$ qubits unaltered. We denote such set as $\mathcal{A}_{\vec{n}_+,\vec{n}_-}$. A sum over all such $2^{N-(n_+ + n_-)}$ states has a common prefactor $(n_\uparrow - m_\uparrow)^2 = (n_+ - n_-)^2$. Note that if not for the modulus square in Eq. (15), such sum would represent a mean of the product of the two operators, namely,

$$\sum_{n,m\in\mathcal{A}_{\vec{n}_+,\vec{n}_-}} \varrho_{nm} = \mathrm{Tr}[\hat{\varrho}\hat{\mathcal{R}}_{\vec{n}_+}\hat{\mathcal{L}}_{\vec{n}_-}]. \tag{20}$$

Using

$$\sum_{i=1}^{2^n}|a_i|^2 \geq \frac{1}{2^n}|\sum_{i=1}^{2^n} a_i|^2 \tag{21}$$

which holds for any 2^n complex numbers [54], we obtain

$$\sum_{n,m\in\mathcal{A}_{\vec{n}_+,\vec{n}_-}} |\varrho_{nm}|^2 \geq \frac{1}{2^{N-(n_+ + n_-)}}\mathcal{E}_{\vec{n}_+,\vec{n}_-} \tag{22}$$

where in correspondence to Eq. (1) we introduced

$$\mathcal{E}_{\vec{n}_+,\vec{n}_-} := |\mathrm{Tr}[\hat{\varrho}\hat{\mathcal{R}}_{\vec{n}_+}\hat{\mathcal{L}}_{\vec{n}_-}]|^2. \tag{23}$$

We plug the inequality (22) into (15) and first sum over all possible combinations of fixed n_+ and n_-, and finally over all n_+ and n_-, obtaining the central expression of this work:

$$F_q \geq 2\sum_{n_+=0}^{N}\sum_{n_-=0}^{N-n_+}\frac{(n_+ - n_-)^2}{2^{N-(n_+ + n_-)}}\sum_{\vec{n}_+,\vec{n}_-}\mathcal{E}_{\vec{n}_+,\vec{n}_-}. \tag{24}$$

Thus the QFI and hence the metrological sensitivity is lower bounded by a combination of $\mathcal{E}_{\vec{n}_+,\vec{n}_-}$, i.e., non-negative Bell correlators of all orders, with non-negative coefficients. Since $\mathcal{E}_{\vec{n}_+,\vec{n}_-} \leq (\frac{1}{4})^{n_+ + n_-}$ for separable states [55], the correlator $\mathcal{E}_{\vec{n}_+,\vec{n}_-}$ is also well suited to quantify the many-body entanglement. Therefore, the result (24) allows one to understand how the depth of the nonlocality or of the entanglement impacts the precision of a quantum sensor [57].

For a pure separable state

$$|\psi\rangle = \bigotimes_{k=1}^{N}\frac{1}{\sqrt{2}}(|\uparrow_k\rangle + |\downarrow_k\rangle), \tag{25}$$

we have $\mathcal{E}_{\vec{n}_+,\vec{n}_-} = (\frac{1}{4})^{n_+ + n_-}$ for all $\vec{n}_+$ and $\vec{n}_-$ (this is a consequence of the spin-permutation symmetry of this state). Hence, the inequality (21) [and thus (22)] is saturated. With this $\mathcal{E}_{\vec{n}_+,\vec{n}_-}$ the sum over $\vec{n}_\pm$ in Eq. (24) can be evaluated, giving the shot-noise scaling of the QFI with the number of qubits $F_q = N$ [note that for pure states, also the inequality (11) is saturated, hence the "=" sign]. To surpass this shot-noise limit it is sufficient that correlators such as $\mathcal{E}_{\vec{n}_+,\vec{n}_-}$ grow by any amount from the entanglement-threshold value $\mathcal{E}_{\vec{n}_+,\vec{n}_-} = (\frac{1}{4})^{n_+ + n_-}$ [52,55], though not necessarily crossing the Bell limit $\mathcal{E}_{\vec{n}_+,\vec{n}_-} = (\frac{1}{2})^{n_+ + n_-}$.

However, many-body nonlocality is sufficient (therefore it is a resource) to give ultrahigh sensitivity. If $\mathcal{E}_{N,0} > \frac{1}{4}(1/2^{m+1})$, at least $N-m$ qubits are Bell correlated [54], and then Eq. (24) gives

$$F_q \geq \frac{N^2}{2^{m+1}}. \tag{26}$$

When the nonlocality extends over the majority of particles, so that m is small, the QFI scales quadratically with N. In particular, when all qubits are nonlocally correlated, then $m = 0$ and

$$F_q \geq \frac{N^2}{2}. \tag{27}$$

The extreme example is the Greenberger-Horne-Zeilinger (GHZ) state

$$|\psi\rangle = \frac{1}{\sqrt{2}}\left(\bigotimes_{k=1}^{N}|\uparrow_k\rangle + \bigotimes_{k=1}^{N}|\downarrow_k\rangle\right), \tag{28}$$

which gives $\mathcal{E}_{N,0} = \mathcal{E}_{0,N} = \frac{1}{4}$, and the QFI saturates the Heisenberg level $F_q = N^2$ [15].

We now illustrate these general considerations with two prominent examples, the Ising chain and a collection of N bosonic qubits. For both cases, we generate the ground state with a corresponding Hamiltonian $\hat{H}$, and take this state as an input of the interferometer, see Eq. (4). In other words, the Hamiltonian $\hat{H}$ is used at the stage of state preparation, while the generator $\hat{h}$ introduces the dependence of θ.

First, we take the antiferromagnetic Ising Hamiltonian with open boundary conditions, i.e.,

$$\hat{H} = U \sum_{j=1}^{N-1} \hat{\sigma}_z^{(j)} \hat{\sigma}_z^{(j+1)} - \sum_{j=1}^{N} \hat{\sigma}_x^{(j)} \tag{29}$$

where U is the strength of the two-body interactions. We take $N = 6, 8, 10, 12, 14$, and 16 and for each N we find the ground state for different $U < 0$. For every U we calculate the QFI using the formula (8) with the generator (5) aligned along the $\xi = z$ axis. On top of this, we evaluate the N-body correlator $\mathcal{E}_{N,0}$ and highlight the values of U for which the correlator detects the many-body nonlocality of the increasing order, see Fig. 1. Clearly, the growing depth of nonlocality is linked with approaching the Heisenberg limit, in accordance to Eq. (26).

As another prominent example we take the collection of N interacting bosonic qubits, such as an ultracold Bose gas in a double-well trap. In the two-mode approximation, such a system can be depicted with the Hamiltonian

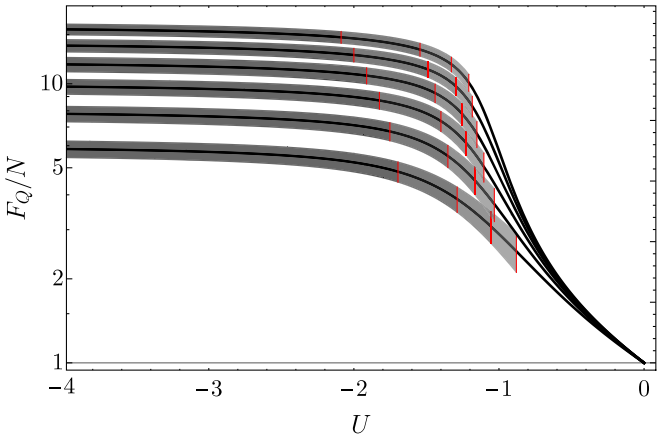

FIG. 1. The QFI, calculated with the ground state of the Hamiltonian (29) and using the generator $\hat{h} = \frac{1}{2}\sum_{k=1}^{N} \hat{\sigma}_z^{(k)}$, as a function of U for $N = 6, 8, 10, 12, 14, 16$ (the higher the plateau the bigger the N) and normalized to the shot noise limit. On top of each curve we marked the regions where the correlator $\mathcal{E}_{N,0}$ detects at least k-partite nonlocality. Therefore, the darkest patch corresponds to $\mathcal{E}_{N,0} > \frac{1}{8}$, when all qubits are Bell correlated. Next, when $\mathcal{E}_{N,0} \in]\frac{1}{16}, \frac{1}{8}]$, so the nonlocality encompasses at least $N-1$ qubits, and so forth. The plot shows that the F_q increases monotonically as the number of nonlocally correlated qubits grows. The red lines separating the regimes with different strength of nonlocality are added for clarity.

$$\hat{H} = -\hat{J}_x + \frac{U}{N}\hat{J}_z^2, \tag{30}$$

where the collective spin operators $\hat{J}_x$ and $\hat{J}_z$ are given by Eq. (5) with $\xi = x$ and $\xi = z$, respectively. The ground state of this system undergoes a quantum phase transition as U passes and drops below -1 [58,59], and when $U \to -\infty$ the ground state approaches the GHZ state (28), which is well suited for our purposes. Figure 2 shows the QFI as a function of U for $N = 50, 100, 250, 500, 750, 1000$ and the correlator $\mathcal{E}_{N,0}$. Again, we observe that when $F_q \simeq N^2$, the system is highly nonlocal. When $N \gg 1$, the $F_q \simeq N^2$ plateau is reached even when $n < N$ qubits are nonlocally correlated because for large N, if a small number of qubits remains uncorrelated, the coefficient $(n_+ - n_-)^2$ from Eq. (24) is still close to N^2. This shows that for $N \to \infty$, while the many-body nonlocality remains sufficient to have high sensitivity, the correlation does not need to encompass all the qubits to have Heisenberg-like scaling.

In Figure 3 we display the correlator $\mathcal{E}_{N,0}$, normalized to the Bell threshold, for the Ising chain (upper panel) and the bosonic case (lower panel) and for two N's: 12, 16, and 100, 150—respectively. The figure shows that the many-body nonlocality emerges in the vicinity of the quantum transition point $U = -1$. The appearance of Bell correlations is accompanied by a rapid growth of the corresponding QFI (see the insets) in accordance to Eq. (24), the main result of this work. Red arrows mark the values of U at which the nonlocality starts to be witnessed by $\mathcal{E}_{N,0}$. These findings contribute to the previous results on the metrological gain in quantum critical systems [60–64] and on the

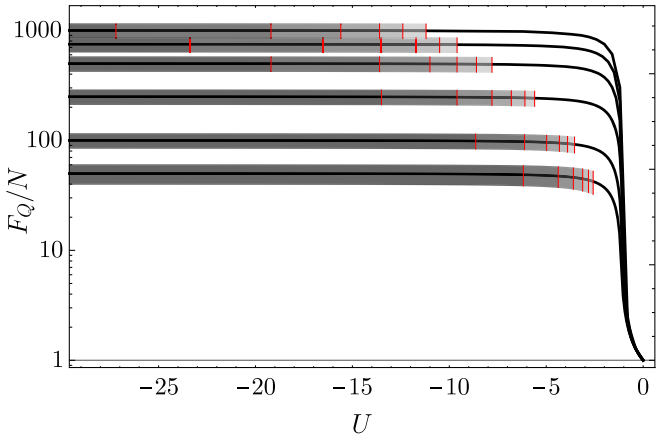

FIG. 2. The QFI, calculated with the ground state of the Hamiltonian (30) and using the collective generator $\hat{h} = \hat{J}_z$, as a function of U for $N = 50, 100, 250, 500, 750, 1000$ (the higher the plateau the bigger the N) and normalized to the shot noise limit. On top of each curve, the full N-body correlator of the highest order is presented with shades of gray, analogically to Fig. 1. For higher N, the Heisenberg level is approached even when $n < N$ qubits are nonlocally correlated.

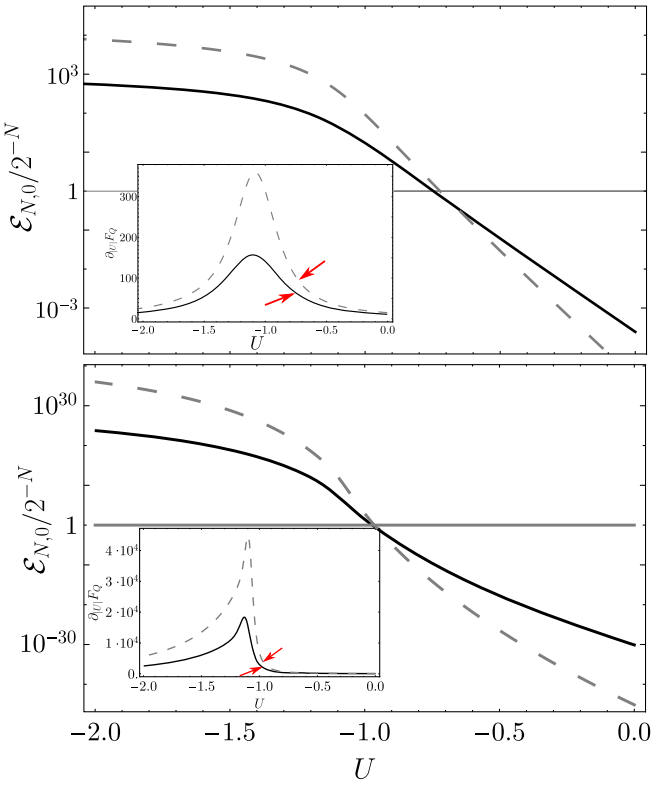

FIG. 3. Upper panel: the correlator $\mathcal{E}_{N,0}$ normalized to the Bell limit 2^{-N}, calculated with the ground state of the Ising Hamiltonian (29) as a function of the interaction strength in the vicinity of the transition point $U = -1$ (solid black line: $N = 12$; dashed grey line $N = 16$). The inset shows the derivative of the QFI for this system, calculated with the same generator $\hat{h}$ as in Fig. 1. The red arrows mark the point at which the correlators cross the nonlocality threshold. Lower panel: same as the upper one, but calculated for the bosonic case and the Hamiltonian (30) (solid black line: $N = 100$; dashed grey line $N = 150$).

emergence of strong quantum correlations in the vicinity of the transition point [65,66].

In conclusion, we have shown that a many-body nonlocality witnessed by the broad family of Bell inequalities from Eq. (2) is a driving mechanism for ultraprecise metrology. We expressed the quantum Fisher information in terms of a combination of a particular set of correlation functions of all orders—such that detect the nonlocality extending over many particles. This central result allows us to provide the lower bound for the sensitivity and identify the necessary condition to reach the Heisenberg scaling of the F_q. These general considerations were illustrated with some prominent examples of multiqubit systems: a collection of spins forming an Ising chain and a gas of ultracold atoms in any two-mode configuration, for instance trapped in a double-well potential. For both cases, we have shown that in the vicinity of a critical point the fast growth of sensitivity is driven by the emerging nonlocality that encompasses an increasing number of particles. Our findings shed some light on the highly nonclassical properties of many-body systems and their implementations.

We acknowledge the support of the National Science Centre, Poland under the QuantERA programme, Project No. 2017/25/Z/ST2/03039.

[1] R. Horodecki, P. Horodecki, M. Horodecki, and K. Horodecki, Rev. Mod. Phys. **81**, 865 (2009).
[2] A. Einstein, B. Podolsky, and N. Rosen, Phys. Rev. **47**, 777 (1935).
[3] Q. Y. He, P. D. Drummond, M. K. Olsen, and M. D. Reid, Phys. Rev. A **86**, 023626 (2012).
[4] E. G. Cavalcanti, S. J. Jones, H. M. Wiseman, and M. D. Reid, Phys. Rev. A **80**, 032112 (2009).
[5] J. S. Bell, Physics **1**, 195 (1964).
[6] N. Brunner, D. Cavalcanti, S. Pironio, V. Scarani, and S. Wehner, Rev. Mod. Phys. **86**, 419 (2014).
[7] A. K. Ekert, Phys. Rev. Lett. **67**, 661 (1991).
[8] L. Chun-Yan, Z. Hong-Yu, W. Yan, and D. Fu-Guo, Chin. Phys. Lett. **22**, 1049 (2005).
[9] J. Barrett, L. Hardy, and A. Kent, Phys. Rev. Lett. **95**, 010503 (2005).
[10] A. Acín, N. Gisin, and L. Masanes, Phys. Rev. Lett. **97**, 120405 (2006).
[11] N. Gisin, S. Pironio, and N. Sangouard, Phys. Rev. Lett. **105**, 070501 (2010).
[12] A. Sørensen and K. Mølmer, Phys. Rev. A **62**, 022311 (2000).
[13] M. Chen, N. C. Menicucci, and O. Pfister, Phys. Rev. Lett. **112**, 120505 (2014).
[14] V. Giovannetti, S. Lloyd, and L. Maccone, Science **306**, 1330 (2004).
[15] L. Pezzé and A. Smerzi, Phys. Rev. Lett. **102**, 100401 (2009).
[16] B. Yadin, M. Fadel, and M. Gessner, Nat. Comm. **12**, 2410 (2021).
[17] F. Fröwis, M. Fadel, P. Treutlein, N. Gisin, and N. Brunner, Phys. Rev. A **99**, 040101(R) (2019).
[18] A. Niezgoda, J. Chwedeńczuk, L. Pezzé, and A. Smerzi, Phys. Rev. A **99**, 062115 (2019).
[19] G. Tóth and T. Vértesi, Phys. Rev. Lett. **120**, 020506 (2018).
[20] S. J. Freedman and J. F. Clauser, Phys. Rev. Lett. **28**, 938 (1972).
[21] A. Aspect, P. Grangier, and G. Roger, Phys. Rev. Lett. **47**, 460 (1981).
[22] A. Aspect, J. Dalibard, and G. Roger, Phys. Rev. Lett. **49**, 1804 (1982).
[23] W. Tittel, J. Brendel, B. Gisin, T. Herzog, H. Zbinden, and N. Gisin, Phys. Rev. A **57**, 3229 (1998).
[24] W. Tittel, J. Brendel, H. Zbinden, and N. Gisin, Phys. Rev. Lett. **81**, 3563 (1998).
[25] G. Weihs, T. Jennewein, C. Simon, H. Weinfurter, and A. Zeilinger, Phys. Rev. Lett. **81**, 5039 (1998).
[26] J.-W. Pan, D. Bouwmeester, M. Daniell, H. Weinfurter, and A. Zeilinger, Nature (London) **403**, 515 (2000).
[27] D. Kielpinski, V. Meyer, C. A. Sackett, W. M. Itano, C. Monroe, and D. J. Wineland, Nature (London) **409**, 791 (2001).

[28] S. Gröblacher, T. Paterek, R. Kaltenbaek, Č. Brukner, M. Żukowski, M. Aspelmeyer, and A. Zeilinger, Nature (London) **446**, 871 (2007).
[29] D. Salart, A. Baas, J. A. W. van Houwelingen, N. Gisin, and H. Zbinden, Phys. Rev. Lett. **100**, 220404 (2008).
[30] B. Hensen, H. Bernien, A. Dréau, A. Reiserer, N. Kalb, M. Blok, J. Ruitenberg, R. Vermeulen, R. Schouten, C. Abellán *et al.*, Nature (London) **526**, 682 (2015).
[31] M. Ansmann, H. Wang, R. C. Bialczak, M. Hofheinz, E. Lucero, M. Neeley, A. D. O'Connell, D. Sank, M. Weides, J. Wenner, A. N. Cleland, and J. M. Martinis, Nature (London) **461**, 504 (2009).
[32] M. Lamehi-Rachti and W. Mittig, Phys. Rev. D **14**, 2543 (1976).
[33] W. Rosenfeld, D. Burchardt, R. Garthoff, K. Redeker, N. Ortegel, M. Rau, and H. Weinfurter, Phys. Rev. Lett. **119**, 010402 (2017).
[34] R. Schmied, J.-D. Bancal, B. Allard, M. Fadel, V. Scarani, P. Treutlein, and N. Sangouard, Science **352**, 441 (2016).
[35] D. K. Shin, B. M. Henson, S. S. Hodgman, T. Wasak, J. Chwedeńczuk, and A. G. Truscott, Nat. Commun. **10**, 4447 (2019).
[36] C. Gross, T. Zibold, E. Nicklas, J. Esteve, and M. K. Oberthaler, Nature (London) **464**, 1165 (2010).
[37] M. F. Riedel, P. Böhi, Y. Li, T. W. Hänsch, A. Sinatra, and P. Treutlein, Nature (London) **464**, 1170 (2010).
[38] I. D. Leroux, M. H. Schleier-Smith, and V. Vuletić, Phys. Rev. Lett. **104**, 250801 (2010).
[39] Z. Chen, J. G. Bohnet, S. R. Sankar, J. Dai, and J. K. Thompson, Phys. Rev. Lett. **106**, 133601 (2011).
[40] J. Esteve, C. Gross, A. Weller, S. Giovanazzi, and M. Oberthaler, Nature (London) **455**, 1216 (2008).
[41] H. Strobel, W. Muessel, D. Linnemann, T. Zibold, D. B. Hume, L. Pezzé, A. Smerzi, and M. K. Oberthaler, Science **345**, 424 (2014).
[42] C. W. Helstrom, Phys. Lett. **25A**, 101 (1967).
[43] C. Helstrom, IEEE Trans. Inf. Theory **14**, 234 (1968).
[44] S. L. Braunstein and C. M. Caves, Phys. Rev. Lett. **72**, 3439 (1994).
[45] S. G. Brush, Rev. Mod. Phys. **39**, 883 (1967).
[46] R. J. Baxter, *Exactly Solved Models in Statistical Mechanics* (Elsevier, New York, 2016).
[47] F. Dalfovo, S. Giorgini, L. P. Pitaevskii, and S. Stringari, Rev. Mod. Phys. **71**, 463 (1999).
[48] Y. Shin, M. Saba, T. A. Pasquini, W. Ketterle, D. E. Pritchard, and A. E. Leanhardt, Phys. Rev. Lett. **92**, 050405 (2004).
[49] R. Gati, B. Hemmerling, J. Fölling, M. Albiez, and M. K. Oberthaler, Phys. Rev. Lett. **96**, 130404 (2006).
[50] M. Żukowski and Č. Brukner, Phys. Rev. Lett. **88**, 210401 (2002).
[51] E. G. Cavalcanti, C. J. Foster, M. D. Reid, and P. D. Drummond, Phys. Rev. Lett. **99**, 210405 (2007).
[52] Q. He, P. Drummond, and M. Reid, Phys. Rev. A **83**, 032120 (2011).
[53] E. G. Cavalcanti, Q. Y. He, M. D. Reid, and H. M. Wiseman, Phys. Rev. A **84**, 032115 (2011).
[54] See Supplemental Material at http://link.aps.org/supplemental/10.1103/PhysRevLett.126.210506 for the details of the derivation.
[55] A. Niezgoda, M. Panfil, and J. Chwedeńczuk, Phys. Rev. A **102**, 042206 (2020).
[56] M. Gessner and A. Smerzi, Phys. Rev. A **97**, 022109 (2018).
[57] P. Hyllus, W. Laskowski, R. Krischek, C. Schwemmer, W. Wieczorek, H. Weinfurter, L. Pezzé, and A. Smerzi, Phys. Rev. A **85**, 022321 (2012).
[58] J. Dziarmaga, A. Smerzi, W. H. Zurek, and A. R. Bishop, Phys. Rev. Lett. **88**, 167001 (2002).
[59] A. Trenkwalder, G. Spagnolli, G. Semeghini, S. Coop, M. Landini, P. Castilho, L. Pezze, G. Modugno, M. Inguscio, A. Smerzi *et al.*, Nat. Phys. **12**, 826 (2016).
[60] C. Invernizzi, M. Korbman, L. C. Venuti, and M. G. A. Paris, Phys. Rev. A **78**, 042106 (2008).
[61] P. Zanardi, M. G. A. Paris, and L. Campos Venuti, Phys. Rev. A **78**, 042105 (2008).
[62] G. Salvatori, A. Mandarino, and M. G. A. Paris, Phys. Rev. A **90**, 022111 (2014).
[63] M. Bina, I. Amelio, and M. G. A. Paris, Phys. Rev. E **93**, 052118 (2016).
[64] L. Garbe, M. Bina, A. Keller, M. G. A. Paris, and S. Felicetti, Phys. Rev. Lett. **124**, 120504 (2020).
[65] A. Piga, A. Aloy, M. Lewenstein, and I. Frérot, Phys. Rev. Lett. **123**, 170604 (2019).
[66] P. Hauke, M. Heyl, L. Tagliacozzo, and P. Zoller, Nat. Phys. **12**, 778 (2016).